Phonon ionization of neutral donors in lightly doped GaAs: A model for the conductance oscillations in semiconductor-insulator-semiconductor tunnel structures

J. P. Leburton
Coordinated Science Laboratory and Department of Electrical and Computer Engineering, University of Illinois, Urbana, Illinois 61801
(Received 18 May 1987)

A model of space-charge generation by phonon ionization of neutral donors in the n-type GaAs layer of the "Hickmott" tunnel device is presented. Various features associated with the periodic structures in the junction conductance, such as peak narrowing in magnetic fields attributed to magnetoimpurity resonance, are explained in terms of one-dimensional LO-phonon emission and ionization rate. The high-temperature data in the experiment of Lu, Tsui, and Cox on In-InP contacts is interpreted in terms of carrier capture by ionized impurities with LO-phonon emission, which is the inverse mechanism of LO-phonon ionization. Theoretical results compare well with the experiment.

I. INTRODUCTION

The observation of conductance oscillations in the presence of magnetic fields in GaAs-$Al_xGa_{1-x}As$-GaAs tunnel structures by Hickmott *et al.*[1-3] has been the subject of controversial interpretations during the last few years.[4-11] The remarkable feature of this anomalous effect is the persistence of oscillations over multiple voltage periods with the period corresponding to the GaAs LO-phonon energy $\hbar\omega_{LO}$. Early experiments in metal-insulator-semiconductor (MIS) tunnel structures have already shown that similar oscillatory effects occur in the absence of magnetic fields.[12,13] Cavenett demonstrated that the conductance oscillations arise from the resistance modulation of the lightly doped semiconducting layer due to the electron-phonon interaction and are enhanced in tunnel structures where the semiconductor resistance is increased with respect to the barrier impedance.[13] Recent experiments performed on MIS structures have confirmed the generality of the oscillatory behavior[8-10] even above nitrogen temperature.[14] It is thus widely accepted that oscillations are related to LO-phonon emission in the lightly doped GaAs buffer layer of the semiconductor-insulator-semiconductor (SIS) tunnel structure. The various interpretations which have been published to account for this effect differ, however, with respect to the specific mechanisms which relate the LO-phonon emission to the conductance oscillations. The following mechanisms have been proposed: ballistic transport,[1] space-charge generation by phonon ionization of neutral donors,[4] charge modulation by slow magneto-polaron formation in high magnetic fields,[5,7] impedance variation by impact ionization of neutral impurities,[8-10] and self-energy correction to the final density of states arising from electron-phonon interaction.[11] Measurements of the temperature dependence of the oscillation amplitude[15] as well as recent experiments using far-infrared spectroscopy strongly suggest an ionization mechanism as responsible for the oscillations.[16]

In some early communications, we interpreted the current oscillations as due more specifically to a space-charge generation by phonon ionization of neutral donors in the GaAs buffer layer.[4] Because of the continuity of the electric field across the $Al_xGa_{1-x}As$-GaAs interface, the space-charge mechanism modifies the electrical state of the undepleted GaAs layer and induces voltage variations across the $Al_xGa_{1-x}As$ tunnel barrier (feedback[5]) which produces periodic current structures when a new sequence of phonon emission is possible, i.e., for $eV_G = M\hbar\omega_{LO}$ where V_G is the gate voltage. In a set of repeated experiments, Eaves and collaborators confirmed the existence of oscillations in the absence of magnetic field, as previously observed in MIS structures,[13] and attributed the magnetic field dependence of the oscillation amplitude to the impedance variation of the undepleted GaAs layer caused by increasing magnetic freezeout. They showed, however, that unlike Hickmott's picture of total freezeout of the buffer layer[1,4,11] a substantial space-charge depletion region exists underneath the tunnel barrier in high magnetic fields. They interpreted the oscillations as caused by an impedance modulation due to impact ionization of neutral donors by energetic electrons injected from the tunnel barrier into the undepleted n-type GaAs buffer layer.[8-10,15,17] The amplitude enhancement and the narrowing of the periodic conductance peak observed around 5 T seems to indicate a magnetoimpurity resonance (MIR) effect which occurs with impact ionization when the separation between Landau levels corresponds to the donor ionization energy.[17] This MIR effect is questionable, however, because one would also observe additional conductance structures, periodic in the magnetic field, as will be shown in Sec. III. It is therefore suitable to examine the contribution of each ionization mechanism (phonon or impact ionization) to the overall charge variation in the n^--type GaAs layer, and explain the multiple features related to the current oscillations.

In the course of investigating the origin of the conduc-

tance oscillations in SIS structures, a major difficulty arises because one deals with an inhomogeneous system which consists of a tunnel barrier on top of a lightly doped layer of semiconducting material. It is not possible to isolate experimentally the contribution of each region of the device to the overall current response or to the total voltage drop across the SIS structure. However the various physical variables (current, electric field, and potential) satisfy continuity conditions which make them interdependent in the different regions.

Because of the large potential variation experienced by the semi-insulating n^--type GaAs layer the voltage drop across the tunnel barrier is only a few percent of the total gate voltage such that LO-phonon emission takes place in the buffer layer of the SIS structure. The central issue is to identify the microscopic process which relates the LO-phonon emission to the mechanism which modulates the current at the barrier injector.

With the presence of space-charge depletion region in the buffer layer,[9] the general scenario leading to the current oscillations consists of three phases (Fig. 1): (1) Electron tunneling and injection across the barrier, (2) electron acceleration with LO-phonon emission in the n-type GaAs high-field region, and (3) microscopic processes causing the current oscillations, with feedback to the tunnel barrier.

The tunnel barrier operates only as a carrier-injection mechanism. The two remaining phases are essential to understand the oscillatory effect. Transport in the high-field buffer layer is important because it determines the energy distribution of carriers entering the undepleted region where conductance oscillations occur. We therefore devote an entire section to this process because several of the previous models[5,9,14] assume velocity phase conservation (velocity coherence) for the carriers in the high-field region, i.e., all the carriers travel the same ballistic distance before emitting a LO phonon in the n^--type GaAs layer, resulting in a significant velocity and energy drop after the emission process. This sawtooth carrier motion would therefore explain the current oscillations because the occurrence of the third phase (Fig. 1) would depend upon the magnitude of the carrier incident energy in the undepleted region. We will see that this picture is too simplistic and that a more elaborated analysis is needed to obtain a good quantitative agreement with the experimental data. In Sec. III, we develop a model of charge generation in the n^--type GaAs layer. The model is based on the distribution of carriers obtained from numerical simulation in the preceding section. We derive the expression for the phonon ionization rate of neutral donors in presence of magnetic field and compare our model with the experimental data. Finally we discuss the interpretation of the MIR effect in connection with our model.

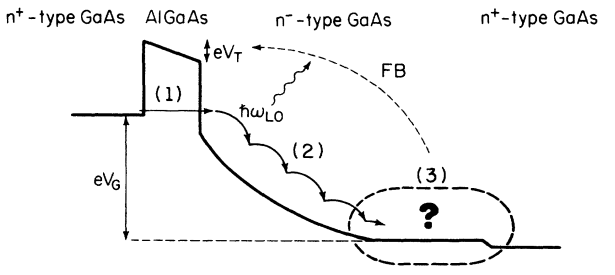

FIG. 1. Schematic representation of the three-phase processes in the n^+-type GaAs-$Al_xGa_{1-x}As$-n^--type GaAs structure at zero-magnetic field: (1) Tunneling process, (2) high-field transport with LO emission, and (3) microscopic process in the neutral region. The dashed FB line represents the feedback to the barrier voltage V_T.

II. HIGH-FIELD TRANSPORT IN THE n^--TYPE GaAs BUFFER LAYER (ZERO-MAGNETIC-FIELD CASE)

The carrier energy distribution in the n^--type GaAs layer of the SIS structure is determined by performing a Monte Carlo simulation of the electron motion in presence of LO-phonon emission. Individual paths of a large number of (4000 in our case) of electrons are simulated using a code which incorporates the nonparabolicity of the band structure.[18] In the absence of magnetic freezeout the n^--type GaAs layer consists of a classical depleted space-charge region and an undepleted quasineutral region extending up to the n^+-type GaAs substrate. We have assumed that the potential V_b in the buffer layer has a classical profile as given by a quadratic expression as a function of the distance W from the $Al_xGa_{1-x}As$ barrier (Fig. 1), i.e., $V_b = eN_DW^2/2\epsilon_S$. Carriers are injected from the left side ($Al_xGa_{1-x}As$ barrier side) with zero velocity and advanced stepwise in time. After each time step, electron positions in real and momentum space are updated. By using this scheme, we keep track of the spatial dependence of scattering statistics and transport variables such as the drift velocity and average energy.

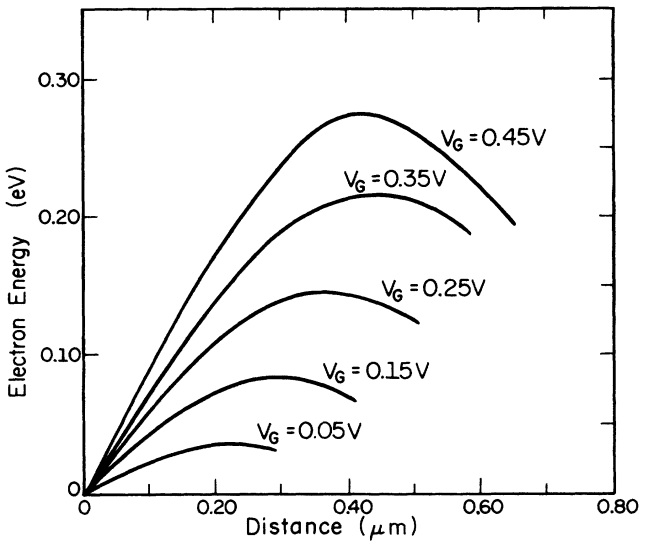

FIG. 2. Electron energy vs distance in the depletion region of the n^--type GaAs layer for different gate voltages. Curves have been terminated when carriers penetrate the undepleted layer (after Wang *et al.* Ref. 18).

In Fig. 2 we have plotted average electron energy as a function of distance in the depletion region for different gate voltages. The curves have been terminated at the end of the depletion region. In the undepleted region, the electron motion is assumed to be a field-free relaxation. As can be seen, oscillatory structures which would reflect the simultaneous stop-and-go carrier motion caused by successive acceleration and phonon emission processes, are entirely absent. This absence of coherence is mostly due to the strength of the electric field which destroys the "phase" among carriers by randomly distributing the individual scattering events. All the curves exhibit an overshoot which varies in position, magnitude, and shape as a function of the gate voltage and the nonuniform electric field in the depletion region. Another important result provided by these numerical data is the value of the carrier energy at the edge of the depletion layer. Carriers penetrate the undepleted region of the GaAs buffer layer with an energy far larger than the phonon energy $\hbar\omega_{LO}$.

Figure 3 shows the electron energy as a function of the gate voltage as the carriers penetrate into the undepleted portion of the n^--type GaAs layer. Two ranges of voltage, the low-bias, $E_G \approx 0.1$ V, and high-bias, $E_G \approx 0.4$ V, regions have been investigated with a finer mesh size. The overall behavior of the carrier energy is a relatively smooth and monotonic function of the gate voltage. For low bias, the detailed calculation (see inset) shows a structure in the energy and velocity characteristics with a period corresponding to the LO-phonon energy. The dips indicate a decrease of the velocity due to the onset of a new LO-phonon emission sequence for low-energy carriers. These carriers have already disposed of all their kinetic energy in the depletion layer, but have been reaccelerated up to an energy corresponding to $\hbar\omega_{LO}$. The dip amplitudes are less than 10 meV and 0.5×10^7 cm/s for energy and drift velocity, respectively, corresponding to amplitude variations of ≈ 15 and $\approx 10\%$. A close look at the carrier distribution function reveals δ-like peaks caused by the LO-phonon emission process (inset). All the peaks in the energy distribution are separated by the well-defined phonon energy $\hbar\omega_{LO}$. The highest-energy peak is located at eV_G and corresponds to ballistic (collision-free) carriers. Only a fraction of the carrier ensemble occupies the lowest level. At high-gate voltage the electron energy decreases because carriers at the edge of the depletion region return to steady-state value after the energy overshoot. The fine structure is barely noticeable. This last result clearly invalidates the concept of velocity coherence.

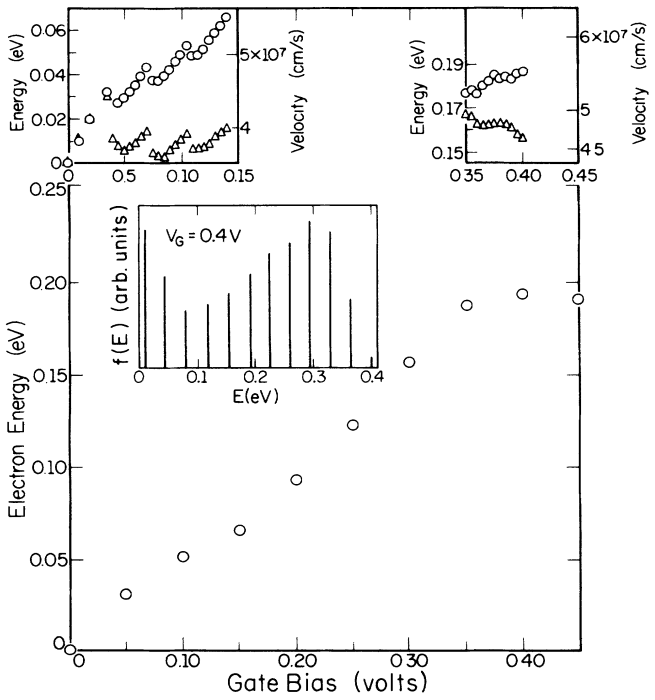

FIG. 3. Electron energy at the edge of the depletion region as a function of the gate voltage. Insets show fine analysis for two voltage ranges (0–0.15 V) and (0.35–0.40 V). ○, energy and △, drift velocity. Also shown is the distribution function $f(E)$ for $V_G = 0.4$ V; the structure period corresponds to $\hbar\omega_{LO}$ (after Wang *et al.* Ref. 18).

At this stage, it is interesting to assess the importance of the space-charge effect produced by the velocity variation as shown in Fig. 3. Owing to current conservation, the variation of the carrier concentration δn resulting from the velocity variation δv_d is given by

$$\delta n = -\frac{J}{e}\frac{\delta v_d}{v_d^2} \tag{1a}$$

or

$$\delta n \approx (2\times10^{10})J \text{ cm}^{-3}, \tag{1b}$$

where J is the current density in A/cm^2 and v_d is the drift velocity. If we assume that this excess charge exists over all the undepleted region of thickness D the resulting electrostatic potential variation is given by

$$\delta V = \frac{1}{2}\frac{e}{\epsilon_S}\delta n D^2 \approx (4\times10^{-3})J \text{ mV} \tag{2}$$

for $D \approx 0.5$ μm. In Hickmott's and Eaves' cases, the current density varies between 10^{-8} and 10^{-5} A/cm^2 and between 10^{-5} and 10^{-1} A/cm^2, respectively.[1,9] Therefore the charge variation is really too small to produce a space-charge effect resulting from electron accumulation in the buffer layer. Similar conclusions have been reached by Eaves and co-workers.[9] Ionization mechanisms have to be invoked to explain the current oscillations.

III. CHARGE GENERATION IN THE n^--TYPE GaAs LAYER

As we mentioned previously, analysis of the high-field transport in the n^--type GaAs depleted region is a necessary step toward a coherent model of ionization of neutral donors since knowledge of the carrier energy distribution provides a direct estimate of the number of particles (electrons or emitted hot phonons) capable of participating in the ionization mechanism. With this in mind, a theory of space-charge generation[4] and impedance varia-

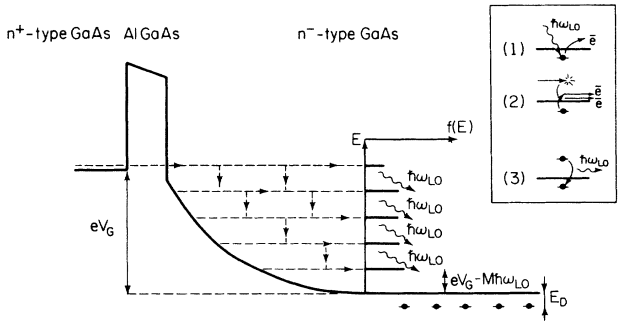

FIG. 4. Schematic energy-band diagram showing the random process of LO-phonon emission in the depleted region of the n^+-type GaAs-$Al_xGa_{1-x}As$-n^--type GaAs structure. The electron distribution function at the entrance of the undepleted region is indicated on a horizontal axis as a function of energy E_D is the donor energy and M is the maximum number of LO phonons emitted by a single carrier. Insets show three fundamental processes: (1) phonon ionization of neutral donors, (2) impact ionization of neutral donors by energetic carriers, and (3) resonant capture of energetic carriers by ionized donors with LO-phonon emission.

tion[9,10] in the undepleted n^--type GaAs region can be formulated

A. Zero-magnetic-field conditions

A schematic cross-sectional view of the tunnel structure with hot-electron mechanisms is shown in Fig. 4. At low temperatures and under reverse bias the lightly doped buffer layer consists of a depletion region and an undepleted layer containing neutral (frozen) donors, which extends up to the n^+-type GaAs substrate.[9] Electrons are injected from the heavily doped GaAs gate through the tunnel barrier into the depletion region with a nearly monoenergetic distribution. Owing to the large electric field across the depletion region an appreciable fraction of electrons are accelerated up to the highest energy $E=eV_G$. Other electrons are scattered by emitting LO phonons resulting in a lower average carrier energy (Fig. 2). However, because of the dispersionless phonon relation, the energy lost $\Delta E=\hbar\omega_{LO}$ in each scattering event is constant. Therefore, the resulting distribution function $f(E)$ (horizontal axis in Fig. 4) of carriers leaving the high-field region is characterized by discrete δ-like peaks separated by the phonon energy $\hbar\omega_{LO}$.[18]

1. Relaxation mechanisms and carrier generation

When carriers penetrate the undepleted region at the right of the energy axis they continue to dispose of their energy by LO-phonon emission but impact ionization of neutral donors [process (2) in Fig. 4 inset] is also possible. The donor ionization rate by impact ionization $1/\tau_{ii}$ is calculated by using the Fermi golden rule

$$\frac{1}{\tau_{ii}}=\sum_{\mathbf{k}_1',\mathbf{k}_2'}\frac{2\pi}{\hbar}|\langle 1',2'|V|1,0\rangle|^2\delta(E_1-E_1'-E_2'-E_D), \tag{3}$$

where $\langle 1',2'|V|1,0\rangle$ is the matrix element of the Coulombic interaction between the incident electron (1 state) and the bound donor state (0 state). The two resulting states after ionization are the 1′ and 2′ plane-wave states. E_1, E_1', and E_2' are the energies of the incident and the resulting states after ionization, respectively. This yields

$$\frac{1}{\tau_{ii}}=\frac{1}{6\pi^2}\frac{N_D^0e^2}{(\epsilon_0\epsilon_S)\hbar}a_B^2F\left[\frac{E}{E_D}\right]. \tag{4}$$

Here, a_B is the donor Bohr radius, m is the electron effective mass, ϵ_S is the dielectric constant, and F is a function of the normalized incident energy E/E_D, where E_D is the donor energy [Fig. 5(a)]. For n^--type GaAs, where $N_D^0\approx10^{15}$ cm^{-3} is the neutral donor concentration[1,10] and $a_B\approx10$ nm, the prefactor is about 6×10^{10} s^{-1}. The ionization F function presents a maximum $F_M\approx0.7$ at $E\approx3.6E_D$ which corresponds to an ionization cross section $\sigma\approx a_B^2$. Notice that the ionization rate strongly decreases at high energies; this implies that only the carriers of the first δ-like peak of the current distribution contribute to the impact ionization. The total scattering cross section is larger due to inelastic Coulombic interactions causing electronic transitions between the donor's hydrogenic levels. The total scattering cross section has been estimated to be as large as $\sigma\approx3\pi a_B^2$, i.e., an order of magnitude larger than the ionization process.[17] However, the LO-phonon emission ($1/\tau_{em}\approx5\times10^{12}$ s^{-1}) remains the only important energy relaxation mechanism in the n^--type GaAs buffer layer.

LO phonons generated by hot carriers are in excess with respect to their equilibrium distribution, and, in turn, are able to ionize neutral donors. The excess LO-phonon population ν is a result of a detailed balance between generation by hot carriers [left-hand side of Eq. (5)] and loss processes due to ionization and decay into acoustic phonons [right-hand side of Eq. (5)], i.e.,

$$\sum_{j=2}^{M+1}\frac{n_j}{\tau_{em}}=\frac{\nu}{\tau_{pi}}+\frac{\nu}{\tau_d}\quad\text{or}\quad\nu=\frac{1}{1/\tau_{pi}+1/\tau_d}\sum_{j=2}^{M+1}\frac{n_j}{\tau_{em}}, \tag{5}$$

where $M+1$ is the total number of δ-like peaks of the distribution function and n_j is the electron concentration of the jth energy peak of the distribution function $f(E)$. The $j=1$ term in the sum does not contribute to the phonon generation because phonon emission is forbidden for $E<\hbar\omega_{LO}$, $1/\tau_d\approx10^{11}$ s^{-1} is the LO-phonon decay rate and $1/\tau_{pi}$ is the donor ionization rate by LO-phonon absorption [process (1) in Fig. 4 inset]. The latter is also calculated using the Fermi golden rule,

$$\frac{1}{\tau_{pi}}=\frac{2\pi}{\hbar}\sum_{\mathbf{k}'}|\langle 0_{ph}|\langle\mathbf{k}|H_{e\text{-}ph}|0\rangle|\mathbf{q}\rangle|^2\times\delta(E(\mathbf{k}')+E_D-\hbar\omega_{LO}), \tag{6}$$

where $H_{e\text{-ph}}$ is the Fröhlich electron-phonon interaction Hamiltonian:[19]

$$H_{e\text{-ph}}=\sum_{q}(C_{\mathbf{q}}a_{\mathbf{q}}e^{i\mathbf{q}\cdot\mathbf{r}}-C_{\mathbf{q}}^{\dagger}a_{\mathbf{q}}^{\dagger}e^{-i\mathbf{q}\cdot\mathbf{r}}) . \tag{7}$$

Here $C_{\mathbf{q}}$ is the coupling parameter given by

$$C_{\mathbf{q}}=i\frac{\hbar\omega_{\mathrm{LO}}}{q}\left[\frac{4\pi}{V}\alpha\right]^{1/2}\left[\frac{\hbar}{2m\omega_{\mathrm{LO}}}\right]^{1/4} , \tag{8}$$

where $\alpha=0.068$ is the Fröhlich coupling constant, $\mathbf{q}$ is the phonon wave vector, and V is the volume of the sample. $C_{\mathbf{q}}^{\dagger}$ is the complex conjugate of $C_{\mathbf{q}}$ and $a_{\mathbf{q}}^{\dagger}$ and $a_{\mathbf{q}}$ are the phonon creation and annihilation operators. In Eq. (6) the $|0\rangle|\mathbf{q}\rangle$ vector is the initial state consisting of the $|0\rangle$ hydrogenic donor state and the occupied $|\mathbf{q}\rangle$ incident phonon states, while the $|\mathbf{k}\rangle|0_{\mathrm{ph}}\rangle$ vector is the combination of the free-electron $|\mathbf{k}\rangle$ states and the nonoccupied $|0_{\mathrm{ph}}\rangle$ phonon state resulting from the donor ionization process. After tedious calculations, we obtain

$$\frac{1}{\tau_{pi}}=\frac{16\pi}{3}N_D^0 a_B\alpha\frac{\hbar}{m}S(qa_B) , \tag{9}$$

where

$$S(x)=\left[\frac{\theta}{x}\right]\left[\frac{1}{\{1+[x-\theta(1-E_D/\hbar\omega_{\mathrm{LO}})^{1/2}]^2\}^3}-\frac{1}{\{1+[x+\theta(1-E_D/\hbar\omega_{\mathrm{LO}})^{1/2}]^2\}^3}\right] . \tag{10}$$

Here $\theta=(2m\omega_{\mathrm{LO}}a_B^2/\hbar)^{1/2}$. With the same parameters as used previously, the prefactor of Eq. (9) is about 2×10^{10} s^{-1}. The S function [Fig. 5(b)] exhibits a maximum $S_M\approx1.5$ at $q\approx0.80(2m\omega_{\mathrm{LO}}/\hbar)^{1/2}$ and an apparent singularity at $q=0$ as a consequence of the $1/q$ dependence of the Fröhlich Hamiltonian and the fact that initial and final states are not orthogonal. Therefore, the phonon ionization rate reaches a maximum value of about 3×10^{10} s^{-1} for $q\approx2\times10^{6}$ cm^{-1}, which corresponds to the wave vector of phonons emitted by energetic carriers at the emission onset. Smaller phonon wave vectors are emitted by electrons of higher energies and thus induce a lower ionization rate. It should be noted that this ionization rate is of the same order of magnitude as the impact ionization rate [process (2) in Fig. 4 inset]. Therefore under electron injection, the total nonequilibrium generation (G) mechanisms consists of three components: thermal generation G_{th}, impact ionization, and donor ionization by LO-phonon absorption, i.e.,

$$G=G_{\mathrm{th}}+\sum_{j=1}^{M+1}\frac{n_j}{\tau_{ii}}+\frac{\nu}{\tau_{pi}} , \tag{11}$$

where ν is given by Eq. (5).

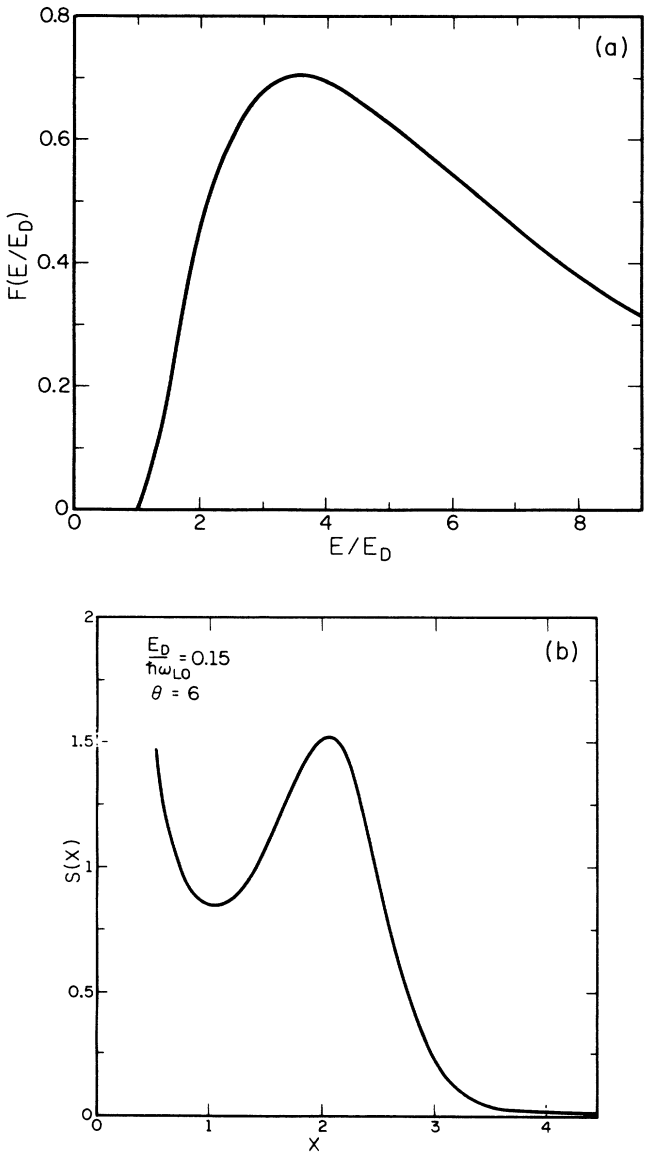

FIG. 5. (a) Plot of the impact ionization F function vs the normalized incident energy E/E_D. (b) Phonon ionization S function vs the normalized phonon wave vector.

2. *Recombination mechanisms*

The nonequilibrium recombination (R) mechanism is the sum of two terms:

$$R=\frac{n_0+\delta n}{\tau_{\mathrm{rec}}}+\frac{n_J}{\tau_c} . \tag{12}$$

The first term is the thermal recombination in the presence of excess carriers δn; n_0 is the equilibrium carrier concentration. The second term is resonant capture by the ionized donors with LO-phonon emission [process (3) in Fig. 4 inset], which occurs only for the first electron level $j=1$, i.e., when

$$E=\hbar\omega_{\mathrm{LO}}-E_D . \tag{13}$$

The capture rate is given by the same expression as Eq. (6) with the sum over $\mathbf{q}$ instead of $\mathbf{k}$,

$$\frac{1}{\tau_c}=\frac{64}{3}\pi^2 N_D^+ a_B^2 \alpha \frac{(\hbar\omega_{LO})^{3/2}}{\sqrt{2m}} \frac{1}{1+k^2a_B^2} \times \left[\frac{3}{8}+\frac{1}{2}\frac{1}{1+k^2a_B^2} + \frac{1}{(1+k^2a_B^2)^2}\right] \delta(E+E_D-\hbar\omega_{LO}) , \quad (14)$$

where the δ-function accounts for the energy conservation during the resonant process and $k=\sqrt{2mE}/\hbar$. At $T=4.2$ K for $N_D-N_A\approx 10^{15}$ cm^{-3}, the free-carrier concentration is $n_0\approx 2\times 10^{13}$ cm^{-3}, which is consistent with a resistivity value $\rho=400\ \Omega$ cm.[9,10] For an acceptor concentration $N_A\approx 2\times 10^{14}$ cm^{-3} the charge neutrality condition yields $N_D^+=N_A^-+n_0\approx 2.2\times 10^{14}$ cm^{-3}. If we assume that the energy width of the $j=1$ resonant peak is $\Gamma_1\approx\hbar\omega_{LO}/50$, we can replace the δ function by $1/\Gamma_1$ and evaluate the capture rate $1/\tau_c\approx 2\times 10^{11}$ s^{-1} at resonance. The choice of Γ_1, is somewhat arbitrary but reasonable for low temperature since the condition for observation of the oscillations is $\hbar\omega_{LO}\gg\Gamma_1$.

3. *Excess carriers in the n$^-$-type GaAs layer*

At steady state, there is a balance between carrier generation and recombination processes. Therefore the resulting excess carrier concentration δn in n^--type GaAs can be calculated. This excess charge concentration varies discretely because by increasing the gate bias, the lowest δ-like peak of the incident distribution function passes the threshold energy for each of the generation or recombination mechanisms (Fig. 4). Monte Carlo simulation shows that for a gate voltage $V_G\approx 0.35$ V, for example, the occupation of the $j=1$ electron state is about $\frac{1}{5}$ of the total electron concentration up to the onset of the second $j=2$ state and then decreases slowly for higher energy. Therefore, the carrier concentration in the lowest δ peaks is $n_1\simeq n_2\approx J/(5ev_d)$ in a first approximation, where $J\approx 7\times 10^{-2}$ A/cm^2 is the current density as provided by the experimental data and $v_d\approx 5\times 10^7$ cm/s is the carrier-drift velocity. With a combination lifetime $\tau_{rec}\approx 7\times 10^{-9}$ s as estimated by Melngailis *et al.*[20] in similar samples, the contribution of the impact ionization mechanism to the excess charge is given by

$$\delta_{n_{ii}}=\frac{1}{5}\frac{J}{ev_d}\frac{\tau_{rec}}{\tau_{ii}}\sim 5\times 10^{11}\ \text{cm}^{-3} . \quad (15)$$

This value is about 2 orders of magnitude smaller than the estimates of Eaves *et al.*[17] who include intra-atomic donor transitions resulting from carrier inelastic scattering in the total ionization rate and assume that by hopping conduction or field ionization, electrons in the donor excited states will contribute to the excess charge. However, the main difference is due to an overestimation of the number of carriers able to impact and ionize the neutral donors at the threshold energy. Eaves *et al.* consider that the current monoenergetic with all the carriers concentrated in the $j=1$ lowest peak of the distribution function, while the random nature of the phonon scattering in n^--type GaAs depleted layer allows only a fraction of them to be in the appropriate energy range for impact ionizing the donors.

The charge variation resulting from LO-phonon ionization and resonant capture with LO-phonon emission are, respectively, given by

$$\delta n_{pi}=\frac{1}{5}\frac{J}{ev_d}\frac{1}{1+\tau_{pi}/\tau_d}\frac{\tau_{rec}}{\tau_{em}}\approx 10^{13}\ \text{cm}^{-3} , \quad (16)$$

$$\delta n_c=-\frac{J}{5ev_d}\frac{\tau_{rec}}{\tau_c}\approx -2\times 10^{12}\ \text{cm} . \quad (17)$$

In Eq. (16) we have considered the excess charge resulting only from the phonons emitted by the second lowest ($j=2$) peak of the distribution function. Additional ionization arises from phonons emitted by high-energy carriers but they do not cause a steplike charge variation.[21] These results indicate that the phonon ionization process is the leading mechanism of charge generation in the undepleted region of the SIS structure. The density of LO phonons emitted by hot carriers exceeds by at least 1 order of magnitude the concentration of electrons able to impact ionize the neutral donors. Notice also that, although depending on the choice of the broadening factor Γ_1, the charge reduction resulting from resonant capture is comparable in magnitude to the charge generated by phonon ionization. This capture mechanism has been found responsible for oscillatory conductivity in diamond[22] and InSb.[23] However, in our case, the situation is more complex because both effects—resonant capture and phonon ionization—occur almost simultaneously since the resonant carrier energy is just a few meV below the threshold energy for phonon emission. The situation is complicated even more by an intermediate regime with subthreshold phonon emission for which the final electron states are the donor excited states. By varying the injection gate voltage near the resonant conditions, the current first decreases due to carrier capture, then, within 3–4 mV, increases again due to the phonon emission onset which causes donor ionization. Therefore the transition range between trapping and ionization is about the width of the peaks in the $\partial^2 I/\partial V_G^2$ curve which corresponds to current minima observed by Guimaraes *et al.*[10] Moreover, the variation of electronic charge during a cycle of carrier trapping ionization over a gate voltage period $\Delta V_G=\hbar\omega_{LO}/e$ is given by $\delta n=\delta n_{pi}-\delta n_c\approx 1.2\times 10^{13}$ cm^3. This results in a relative resistance variation $\Delta R/R=\delta n/(n_0+\delta n)\approx 0.3$ which is in good agreement with the experimental data.[9] This resistance variation in turn corresponds to a voltage drop $\delta V_u=\Delta RI\approx 0.4$ mV$\approx kT/e$ in the undepleted region and thus induces a variation of the $Al_xGa_{1-x}As$ barrier field $\Delta F_T/F_T=\Delta RI/WF_T\approx 10^{-3}$ (W is the depletion width) which modulates the tunnel current.

The model is consistent with the high-temperature data of Lu, Tsui, and Cox.[14] In this case, the high current density produces complete and uniform background ionization. However the periodic capture mechanism can persist above the freezeout temperature when periodic ionization vanishes. Although the low-energy carrier dis-

tribution n_1 is broader than a few meV and thus reduces the capture rate in Eq. (14), charge trapping is still important since the current density is several orders of magnitude 10^3-10^4 larger than in the previous experiment, resulting in an appreciable resistivity variation in the undepleted layer, as seen from Eq. (17).

B. Nonzero magnetic field conditions

In Hickmott's experiment the conductance oscillations are enhanced by the presence of magnetic fields.[1,3] For instance, the voltage variation during an oscillation cycle $\delta V = V_G \Delta I / 2I \approx 3.5$ mV, as estimated from the relation $I \propto V_G^2$, established by Hellman *et al.*[5] (data at $H = 12$ T with $\Delta I / I \approx 2 \times 10^{-2}$ for $V_G = 0.35$ V) is more than 1 order of magnitude larger than the thermal voltage $kT/e \approx 0.14$ mV ($T \approx 1.6$ K) and consequently cannot be attributed to an *Ohmic* resistance variation of the undepleted (neutral) region, as suggested by several authors.[5,9]

We attribute this voltage variation to space-charge effects which modify the electric field profile in the GaAs undepleted region. A calculation of the residual electric field yields $\delta F = \delta V / D \simeq 100$ V/cm where $D = L - W \approx 0.35$ μm is the width of the undepleted layer and $W \approx 0.65$ μm is the extension of the depletion region at $V_G \approx 0.35$ V. This electric field variation is compatible with the existence of magnetic freeze out in the undepleted region since field ionization of neutral donors occurs at higher-electric fields. Therefore LO-phonon ionization takes place and releases the frozen electrons from the neutral donors resulting in a space-charge effect which reduces the potential drop in the GaAs buffer layer and consequently increases the $Al_xGa_{1-x}As$ barrier field causing a tunnel current enhancement. The LO-phonon ionization rate with electron states modified by the magnetic field is calculated in a manner similar to that of previous sections.

In longitudinal magnetic fields, the electron wave function in the conduction band is given by

$$\Psi_c = \left[\frac{eH}{2\pi\hbar c}\right]^{1/2} \frac{1}{\sqrt{L}} \exp\left[-\left[\frac{eH}{4\hbar c}(x^2+y^2) - ik_z z\right]\right], \tag{18}$$

where H is the magnetic field in the z direction, and k_z is the longitudinal wave vector. Here, for the sake of simplicity, we only consider the lowest Landau level of the conduction band.

The ionization energies of shallow hydrogenic donors in magnetic field were first calculated by Yafet, Keyes, and Adams (YKA) with a variational method.[24] Later Larsen[25] improved the model by using trial wave functions which yield more accurate ionization energies.[26] However, in the former method the donor wave functions are more practical for analytical purposes. Moreover in the range of magnetic fields achieved in the experiment, the ionization energies are not significantly lower than Larsen's results ($< 10\%$). Therefore, in the following derivation, we will use a hybrid method combining the YKA wave functions and Larsen's energies to calculate the phonon ionization rate.

The YKA donor wave function is given by

$$\Psi_i = \frac{1}{(2\pi)^{3/4}(a_\perp^2 a_z)^{1/2}} \exp\left[-\left[\frac{(x-x_i)^2+(y-y_i)^2}{4a_\perp^2} + \frac{(z-z_i)^2}{4a_z^2}\right]\right], \tag{19}$$

where $a_\perp$ and a_z are the variational parameters and $\mathbf{r} = (x_i, y_i, z_i)$ is the position of the donor atom. Again, we assume that only the lowest donor state is occupied under magnetic freezeout.

The electron-phonon interaction Hamiltonian is given by Eq. (7). After integration, the electron-phonon matrix element is

$$M = 2^{7/4}\pi^{1/4} \frac{C_q}{\sqrt{L}} \frac{a_\perp (a_z)^{1/2}}{[1+(a_\perp/a_c)^2]a_c} \exp\left[-\left[\frac{q_\perp^2 a_\perp^2}{1+(a_\perp/a_c)^2} + (k_z - q_z)^2 a_z^2\right]\right] \times \exp\left[-\left[\frac{x_i^2+y_i^2}{4(a_c^2+a_\perp^2)} - \frac{iq_x x_i + iq_y y_i}{1+(a_\perp/a_c)^2} - i(k_z - q_z)z_i\right]\right], \tag{20}$$

with $a_c = \hbar c / eH$. This matrix element describes the absorption of a phonon by a bound electron at a distance $|\mathbf{r} - \mathbf{r}_i|$ from the center of the donor atom. Here $q_\perp$ is the component of the phonon wave vector perpendicular to the magnetic field. In this model it as assumed that the donor center is not necessarily on the path of the traveling phonon. The transition probability for the ionization process and the total ionization rate are given by

$$W_i(k_z, \mathbf{q}) = \frac{2\pi}{\hbar} M^2(\mathbf{q}) \delta\left[\frac{\hbar^2 k_z^2}{2m} + E_D - \hbar\omega_{LO}\right] \tag{21}$$

and

$$\frac{1}{\tau} = \sum_i \sum_{k_z} W_i(k_z, \mathbf{q}), \tag{22}$$

where the summation is carried out over all the longitudinal wave vectors k_z and all the impurity indices i. We next make the transformation from discrete to continuous variables

$$\sum_{k_z} \rightarrow \xi H \frac{L}{2\pi} \int dk_z \ , \tag{23a}$$

$$\sum_{i} \rightarrow N_D^0 \int d\mathbf{r}_i \ , \tag{23b}$$

where ξH is the degeneracy of the Landau levels and N_D^0 is the neutral donor concentration. We finally obtain the ionization rate for LO phonons:

$$\frac{1}{\tau_{\rm LO}} = \frac{16}{\sqrt{2}} \pi^{3/2} N_D^0 \frac{a_z}{1+(a_c/a_\perp)^2} \alpha \frac{\hbar}{m} \frac{1}{(1-E_D/\hbar\omega_{\rm LO})^{1/2}} S^H(q_\perp, q_z) \ , \tag{24}$$

where

$$S^H(q_\perp, q_z) = \frac{2m\omega_{\rm LO}}{\hbar q^2} \exp\left[-2\frac{q_\perp^2 a_\perp^2}{1+(a_\perp/a_c)^2}\right] \{\exp[-2(k_c-q_z)^2 a_z^2] + \exp[-2(k_c+q_z)^2 a_z^2]\} \tag{25}$$

and

$$k_c = \left[\frac{2m\omega_{\rm LO}}{\hbar}\left[1-\frac{E_D}{\hbar\omega_{\rm LO}}\right]\right]^{1/2} .$$

Table I gives the values of the different parameters for $\gamma = \hbar\omega_c/2\mathcal{R} = 1$ and 2 corresponding to magnetic field amplitudes $H = 6.5$ and 13 T, respectively. Here ω_c is the cyclotron frequency and $\mathcal{R}$ is the Rydberg constant. The expression of the ionization rate is similar to Eq. (10). By using the parameters of Table I, it is easily seen that the prefactor is virtually unchanged with respect to zero-magnetic-field conditions. The ionizations S^H function, however, is different from the expression in Eq. (10). A well-defined peak is now identified at $q_z a_z \approx \pm 2$ for low-magnetic fields (Fig. 6). The pronounced minimum at low wave vector is a unique feature of the one-dimensional (1D) character of the electron wave function, which results from confinement caused by the magnetic field. It is a real effect which is independent of the choice of the trial wave function. For high magnetic field, the position of the peaks are shifted toward low wave vectors and are less pronounced because of the influence of the $1/q^2$ singularity in the LO-phonon scattering rate. For the range of magnetic fields considered in this experiment, i.e., $H \leq 14$ T, the maxima are still well resolved and thus limits the ionization process to a small range of phonon wave vectors around the peaks, i.e., for $q_z \approx \pm k_c$. This is a consequence of energy conservation during the electron-phonon interaction.

In addition to this particular behavior of the ionization rate, the 1D LO-phonon density exhibits features different from the 3D (zero-magnetic-field) conditions. As a generalization of Eq. (5), the density ν of LO phonons emitted by hot carriers in the GaAs undepleted layer is given by the relation

$$\nu \propto \sum_{j=2}^{M+1} \int_{\hbar\omega_{\rm LO}}^{\infty} \frac{dE}{\tau_{\rm em}(E)} N(E) \times f_j(eV_g - (M+1-j)\hbar\omega_{\rm LO} - E) \ , \tag{26}$$

TABLE I. Numerical values of the parameters used in the calculations: $\gamma = \hbar\omega_c/2\mathcal{R}$ where ω_c is the cyclotron frequency and $\mathcal{R}$ is the Rydberg constant equal to 5.8 meV; a_z and $a_\perp$ are from Ref. 15, E_D is the ionization energy from Ref. 28, and $a_c = \sqrt{\hbar c/eH}$ is the cyclotron radius.

γ	a_z (Å)	$a_\perp$ (Å)	a_c (Å)	E_D (units of $\mathcal{R}$)
1	73	59	98	1.66
2	65	49	69	2.04

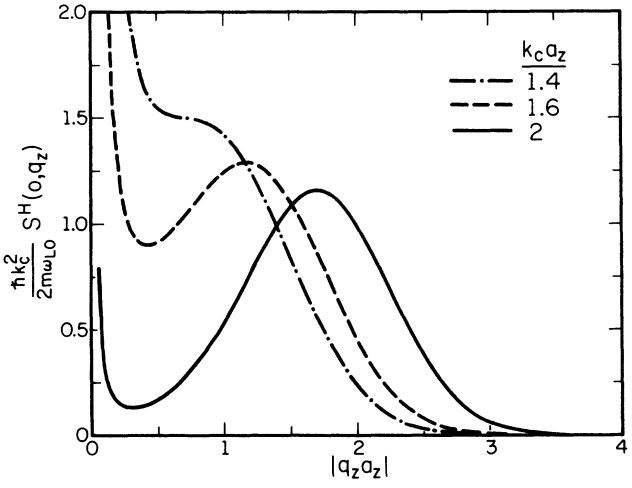

FIG. 6. Magnetic field dependent phonon ionization S^H function vs the normalized z component of the absolute value of the phonon wave vector $q_z a_z$, for different values of the parameter $k_c a_z$ decreasing with magnetic fields. From Table I, $k_c a_z = 1.6$ for $H = 6$ T. For comparison the limiting case $H = 0$ corresponds to $k_c a_z = 2.3$.

$N(E)$ is the electron density of states and f_j is the mini-distribution of electrons around the jth peak of the total $f(E)$ distribution represented in Fig. 4. If for the sake of simplicity we assume a Gaussian shape characterized by a broadening parameter Γ, i.e.,

$$f_j \propto n_j \exp\left[-\frac{[eV_G-(M+1-j)\hbar\omega_{\rm LO}-E]^2}{\Gamma^2}\right] \quad (27)$$

and if we neglect the weak variation of the n_j coefficients with the j parameter, the dependence of the number of LO phonons ν on the gate voltage has a profile shown in Fig. 7 for zero (3D) and nonzero (1D) magnetic fields. The second derivatives $d^2\nu/dV_G^2$ of the 3D curve shows sharp maxima for $V_G=M\hbar\omega_{\rm LO}/e$ which correspond to the onset of a new sequence of phonon emission when the lowest peak in the hot-carrier $f(E)$ distribution function crosses the threshold energy $E=\hbar\omega_{\rm LO}$.

In the presence of magnetic fields, owing to the singular nature of the 1D density of states, the trace in the second derivative changes as shown in Fig. 7 (b). The maximum peak becomes much higher and narrower [the vertical scales in Fig. 7(b) have been reduced to accommodate the $d^2\nu/dV_G^2$ curve] and is followed by a pronounced minimum. This behavior which is a characteristic of the LO-phonon density and thus of the phonon ionization process is observed in the experimental data. Hence, in Fig. 8, the experimental peak at $V_G\approx 155$ mV (Ref. 17) changes from a sharp maxima at zero-magnetic field to a shape similar to that predicted by our theory at $H=5.5$ T. In our calculation, we have assumed that the broadening factor Γ is constant and equal to the $H=0$

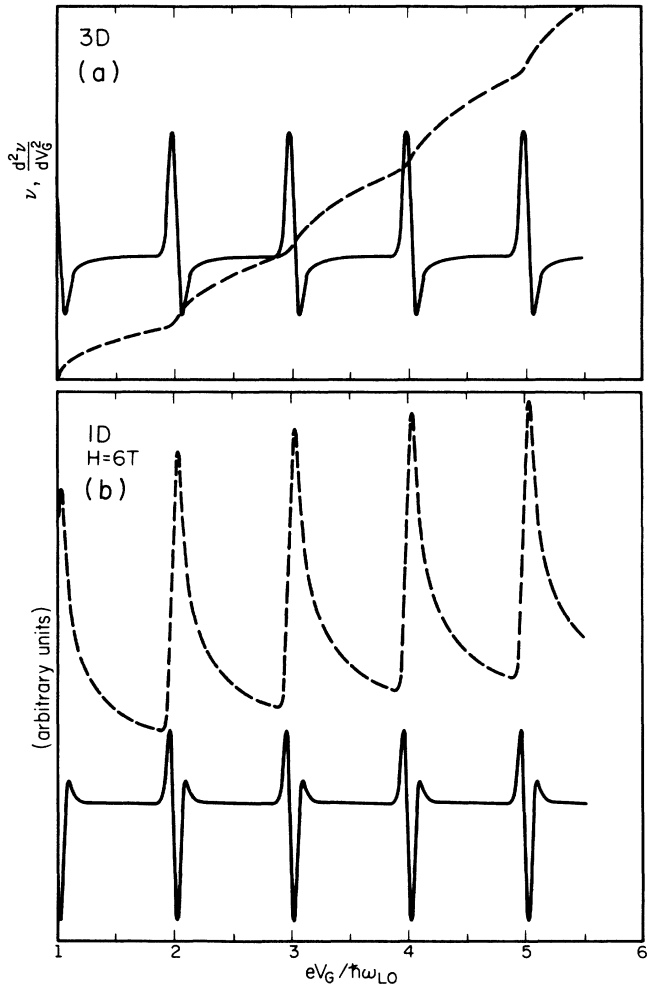

FIG. 7. Plot of the LO-phonon density ν and $d^2\nu/dV^2$ vs the gate voltage V_G as derived from Eq. (32). (a) Zero magnetic field (3D) and (b) nonzero magnetic field (1D) cases. The broadening factor is $\Gamma=\hbar\omega_{\rm LO}/20$.

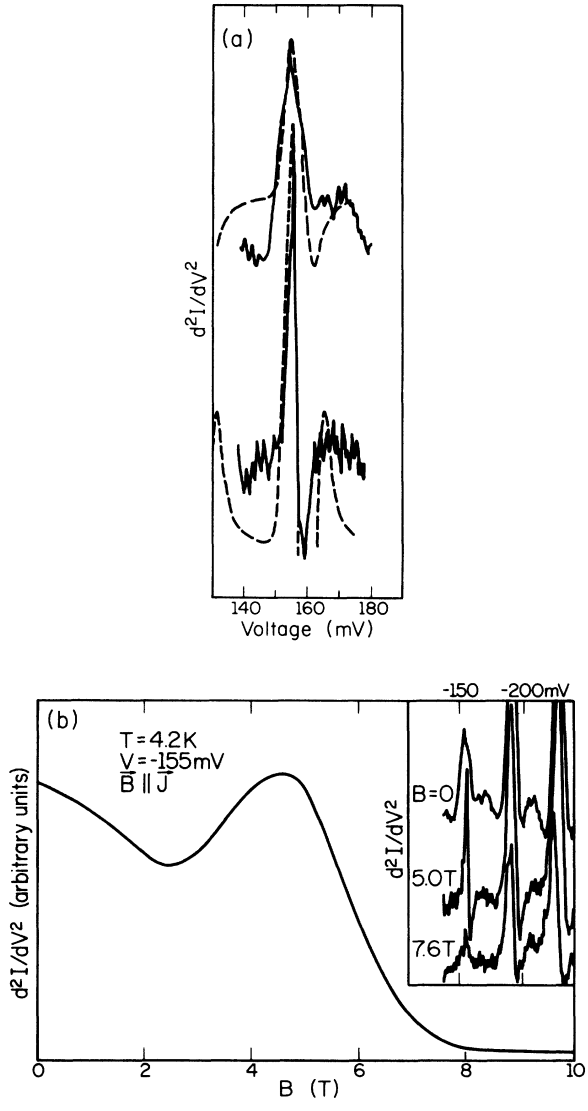

FIG. 8. (a) Shape variation of the LO-phonon peak at $V_G\simeq 155$ mV; in the d^2I/dV_G^2 curve at 4.2 K, showing the narrowing and amplitude enhancement with magnetic field. Upper curve, $H=0$; lower curve, $H=5$ T from Ref. 14. The dashed lines shows the theoretical curve calculated from phonon emission. (b) Trace of the d^2I/dV_G^2 peak as a function of magnetic field.

experimental value. In both cases, $H=0$ and $H\neq 0$, the amplitude of the d^2v/dV_G^2 curves have been fitted with the experimental data. Consequently, the characteristic shape of the second derivative peak exhibits the LO-phonon signature in the charge ionization process.

The above effect has been attributed to a magnetoimpurity resonance (MIR) which occurs when the separation $\hbar\omega_c$ between Landau levels is equal to the donor ionization energy $E_D(H)$. For this condition, the ionization energy corresponds to the joint density of states which is maximum for hot electrons falling from the $p=1$ to $p=0$ Landau level. The occurrence of the MIR effect seems to demonstrate impact ionization in the charge generation in the neutral semiconductor layer.[17] Otherwise, if the LO-phonon ionization mechanism were dominant, one would observe magnetophonon oscillations in the d^2I/dV^2 peak amplitude when the condition

$$\hbar\omega_{\mathrm{LO}}=N\hbar\omega_c+E_D(H) \tag{28}$$

is satisfied, with N being an integer. Here ω_c is the cyclotron frequency. This argument is questionable because there is no reason to restrict the MIR mechanism to hot-electron transitions between the first two Landau levels. Non-negligible higher-order resonance transitions have been experimentally evidenced.[27] Therefore, the resonance should also occur for transitions between higher successive Landau levels, i.e., when $(p'-p)\hbar\omega_c=E_D(H)$ with $p'p\gg 1$ but $\Delta p=p'-p=1$ (Fig. 9). Because the occupation of the higher Landau levels is a function of the injection energy in the n^--type GaAs undepleted neutral layer, current structures with periodicity $\Delta V_G=\hbar\omega_c/e$, should appear in the conductance characteristics.

By contrast to impact ionization, phonon ionization involves a well-defined energy constant

$$\hbar\omega_{\mathrm{LO}}=E_D(H)+E_p(k_z) \tag{29}$$

and thus occurs with an unique voltage period $\delta V_G=\hbar\omega_{\mathrm{LO}}/e$, which is effectively observed. Here $E(k_z)$ is the residual kinetic energy of the emitted carriers in the p Landau level and k_z the electron wave vector. Furthermore, as shown previously phonon ionization dominates the impact ionization mechanism because the density of hot phonons exceeds the density of hot carriers by at least 1 order of magnitude. This results from the LO mode low-group velocity ($v^{\mathrm{ph}}\approx 0$) which causes the phonons to pile up ($\tau_{\mathrm{ph}}\approx 10^{-11}$ s) in the undepleted region until decaying. By comparison, hot carriers spend a shorter time $\tau_t=D/v_d\approx 10^{-12}$ s in the undepleted region ($D\approx 0.5$ μm is the undepleted width, and $v_d\approx 5.10^7$ cm/s is the carrier-drift velocity) and, consequently, are in low concentration. Therefore the impact ionization mechanism seems to be absent in this case, and the features (peak narrowing and amplitude enhancement) observed in the trace of the current structures, are due to the particular conditions which determine the observation of the phonon ionization process in presence of magnetic field. Hence the broad maximum observed in the peak amplitude of the d^2I/dV^2 curves around 5 T may be due to a tradeoff between a peak enhancement due to the 1D nature of the phonon emission process as shown previously

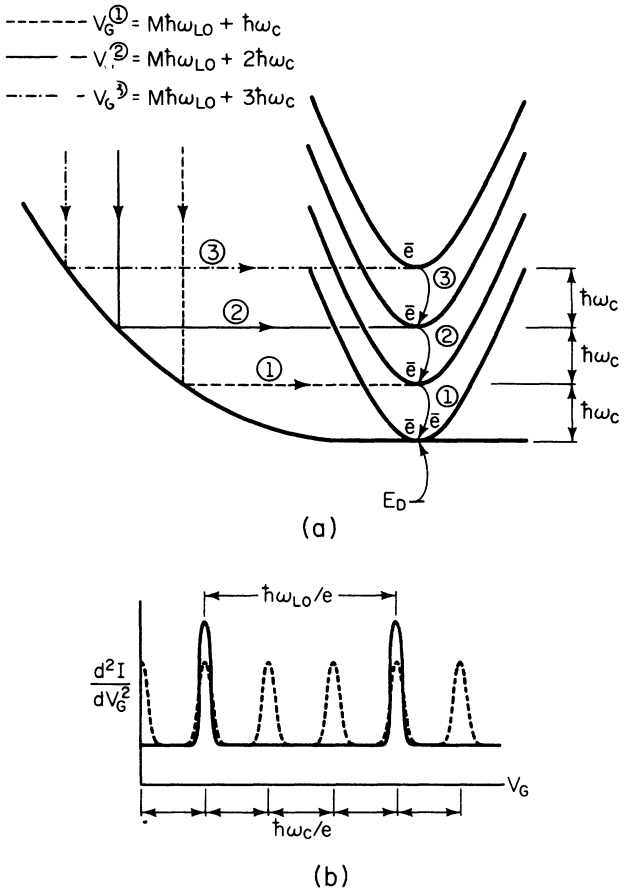

FIG. 9. (a) Conduction-band edge at the transition between depleted and undepleted regions of n-type GaAs, showing schematically three injection conditions of hot carriers resulting in three MIR processes involving different Landau levels. (b) Expected MIR periodic structures (dashed line) superimposed to the zero-magnetic-field LO-phonon peaks (solid line). Here $\hbar\omega_{\mathrm{LO}}=3\hbar\omega_c$.

and a decreasing current density which reduces the number of ionizing particles and thus suppresses the oscillations at high magnetic fields.[10]

IV. CONCLUSIONS

The basic features of the conductances oscillations in SIS tunnel structures have been explained by a mechanism of space-charge generation caused by phonon ionization of neutral donors in the lightly doped GaAs layer of the structure. The ionization mechanism is modulated by the gate voltage which determines the maximum number of phonons M emitted by each carrier when $eV_G=M\hbar\omega_{\mathrm{LO}}$, the potential variation resulting from the periodic charge generation feeds back to the $Al_xGa_{1-x}As$ tunnel barrier and induces the observed current oscillations. Other processes such as impact ionization and carrier capture by ionized impurities with LO-phonon emission are possible but appear less impor-

tant. In the experiments of Lu, Tsui, and Cox on In-InP contacts, the persistence of the oscillations up to 77 K seems to exclude periodic donor ionization since the high temperature and high-current density cause uniform and complete background ionization. Periodic carrier capture with subthreshold LO-phonon emission can still be appreciable, and result in resistance variation which persists at high temperature in the lightly doped InP layer. At this stage, however, direct and quantitative comparison of our model with experimental data is difficult because of the uncertainty affecting certain parameters as the doping level and the recombination rate in InP for example. More detailed experimental data are needed to confirm the generality of this model.

ACKNOWLEDGMENTS

We are indebted to T. W. Hickmott for providing us with his experimental data. We are also grateful to K. Hess, G. E. Stillman, and B. Mason for valuable discussions. We also wish to thank Mrs. E. Kesler and C. Willms, S. Briggs and D. Baily for technical assistance. This work was supported by the Joint Services Electronics Program under Contract No. N00014-84-C-0148.

[1]T. W. Hickmott, P. M. Solomon, F. F. Fang, F. Stern, R. Fischer, and H. Morkoç Phys. Rev. Lett. **52**, 2053 (1984).

[2]T. W. Hickmott, P. M. Solomon, F. F. Fang, R. Fischer, and H. Morkoç, in *Proceedings of the 17th International Conference on the Physics of Semiconductors, San Francisco, 1984,* edited by J. D. Chadi and W. A. Harrison (Springer-Verlag, New York, 1985), p. 417.

[3]T. W. Hickmott, Phys. Rev. B **32**, 6531 (1985).

[4]J. P. Leburton, Phys. Rev. B **31**, 4080 (1985); Physica B + C **134B** (1985).

[5]E. S. Hellman, J. S. Harris, C. B. Hanna, and R. B. Laughlin, Physica B + C **134B**, 41 (1985).

[6]E. S. Hellman and J. S. Harris, Phys. Rev. B **33**, 8284 (1986).

[7]C. B. Hanna and R. B. Laughlin, Phys. Rev. Lett. **56**, 2547 (1986).

[8]L. Eaves, P. S. S. Guimaraes, B. R. Snell, D. C. Taylor, and K. Singer, Phys. Rev. Lett. **55**, 262 (1985).

[9]L. Eaves, P. S. S. Guimaraes, F. W. Sheard, B. R. Snell, D. C. Taylor, G. A. Toombs, and K. Singer, J. Phys. C **18** L885 (1985); see also D. C. Taylor, P. S. S. Guimaraes, B. R. Snell, L. Eaves, F. W. Sheard, G. A. Toombs, and K. Singer, Physica B + C **134B**, 12 (1985).

[10]P. S. S. Guimaraes, D. C. Taylor, B. R. Snell, L. Eaves, K. E. Singer, G. Hill, M. A. Pate, G. Toombs, and F. W. Sheard, J. Phys. C **18**, L605 (1985).

[11]J. Ihm, Phys. Rev. **55**, 999 (1985); Phys. Rev. Lett. **56**, 2548 (1986).

[12]Y. Katayana and K. F. Komatsubara, Phys. Rev. Lett. **19**, 1421 (1967).

[13]C. Cavenett, Phys. Rev. B **5**, 3049 (1972).

[14]P. F. Lu, D. C. Tsui, and H. M. Cox, Phys. Rev. Lett. **54**, 1563 (1985); Bull. Am. Phys. Soc. **31**, 394 (1986).

[15]D. C. Taylor, P. S. S. Guimaraes, B. R. Snell, L. Eaves, F. W. Sheard, G. A. Toombs, J. C. Portal, L. Dmowski, K. E. Singer, G. Hill, and M. A. Pate, Surf. Sci. **174**, 472 (1986).

[16]P. M. Campbell, J. Comas, R. J. Wagner, and J. E. Furneaux, Bull. Am. Phys. Soc. **32**, 886 (1987).

[17]L. Eaves, B. R. Snell, D. K. Maud, P. S. S. Guimaraes, D. C. Taylor, F. W. Sheard, G. A. Toombs, J. C. Portal, L. Dmowski, P. Claxton, G. Hill, M. A. Pate, and S. J. Bass, in *Proceedings of the 18th International Conference on the Physics of Semiconductors, Stockholm, 1986,* edited by O. Engström (World Scientific, Singapore, 1987), pp. 1615–1622.

[18]T. Wang J. P. Leburton, K. Hess, and D. Bailey, Phys. Rev. B **23**, 2906 (1986).

[19]See, e.g., R. Evrard in *Polarons in Ionic Crystals and Polar Semiconductors* edited by J. T. Devreese (North-Holland, Amsterdam, 1972), pp. 29–80.

[20]I. Melngailis, G. E. Stillman, J. O. Dimmock, and C. M. Wolfe, Phys. Rev. Lett. **23**, 1111 (1969).

[21]The carrier distribution varies spatially in the undepleted layer which may affect these estimations. However, due to the high injection velocity from the high-field region, carriers undergo only a few scattering events, mostly LO-phonon emission, during their short flight (less than 1 ps) to the substrate. This is insufficient to completely relax the carrier distribution to equilibrium which requires longer distances, especially for high-energy carriers. The average distance for phonon emission is $d \sim 0.1$ μm so that the emission of n phonons requires an nd distance [J. A. Kash, J. C. Tsang, and J. M. Hvam, Phys. Rev. Lett. **54**, 2151 (1985)]. For the injection condition $V_g = 0.35$ V assumed in our calculation, the energy distribution spreads over ten phonon energies and relaxes at least over a distance of 1 μm, which is three times longer than the undepleted n^--type GaAs layer $[D - (2\epsilon_s V_g / qN_a)^{1/2} = 0.33$ μm for $N_a \approx 10^{15}$ cm$^{-3}]$. Therefore in average, the occupation of the first δ-like peaks may change by a factor of 2, but this affects equally the three processes as seen from Eqs. (15)–(17), so that their relative importance remains the same.

[22]J. R. Hardy, S. D. Smith, and W. Taylor, in *Proceedings of the Institute Conference on the Physics of Semiconductors, Exeter, 1962* (Institute of Physics and Physical Society, London, 1962), pp. 521–528.

[23]H. J. Stocker, H. Levinstein, and C. R. Stannard, Phys. Rev. **150**, 613 (1966).

[24]Y. Yafet, R. W. Keyes, and E. N. Adams, J. Phys. Chem. Solids **1**, 137 (1956).

[25]D. M. Larsen, J. Phys. Chem. Solids **29**, 271 (1968).

[26]G. E. Stillman, C. M. Wolfe, and J. O. Dimmock, in *Semiconductors and Semimetals,* edited by R. K. Willardson and A. C. Beer (Academic, New York, 1977), Vol. 12, pp. 169.

[27]L. Eaves and J. C. Portal, J. Phys. C **12**, 2809 (1979).